Thermodynamic and Nonstoichiometric Behavior of the GdBa$_2$Cu$_3$O$_x$ System*

by

M. Tetenbaum, D. Diana, B. S. Tani, and M. Blander
Chemical Technology Division
Argonne National Laboratory
9700 South Cass Avenue
Argonne, Illinois 60439

September 1998

For Publication in the Proceedings of the First China International Conference on High Performance Ceramics, Oct. 31-Nov. 3, 1998, Beijing, China

DISCLAIMER

DISCLAIMER

Portions of this document may be illegible
in electronic image products. Images are
produced from the best available original
document.

Thermodynamic and Nonstoichiometric Behavior of the $GdBa_2Cu_3O_x$ System.

Marvin Tetenbaum, Dan Diana, Benjamin S. Tani, and Milton Blander

Chemical Technology Division, Argonne National Laboratory,
9700 South Cass Avenue, Argonne, Illinois 60439, USA

Electromotive force (EMF) measurements of oxygen fugacities as a function of stoichiometry have been made on the $GdBa_2Cu_3O_x$ system in the temperature range ~400-600°C by means of an oxygen titration technique with an yttria-stabilized zirconia electrolyte. Equations for the variation of oxygen partial pressure with composition and temperature have been derived from our EMF measurements. The shape of the 400°C isotherms as a function of oxygen stoichiometry for the Gd and Nd cuprate systems suggests the presence of miscibility gaps at values of x that are higher than those in the $YBa_2Cu_3O_x$ system. For a given oxygen stoichiometry, oxygen partial pressures above Gd-123 and Nd-123 cuprate systems are higher (above x = 6.5) than that for the Y-123 system.

A thermodynamic assessment and intercomparison of our partial pressure measurements with the results of related measurements will be presented.

1. INTRODUCTION

The objective of our present study is to investigate the nonstoichiometric and thermodynamic behavior of the high-Tc superconductor oxide system, $GdBa_2Cu_3O_x$ (Gd-123), as a function of oxygen partial pressure, oxygen stoichiometry, and temperature. It should be noted that renewed interest in the $YBa_2Cu_3O_x$ (Y-123) system and related rare-earth systems has occurred because of promising developments of coated conductors which can yield significantly higher current densities than the $Bi_2Sr_2CaCu_2O_x$ (Bi-2212) and lead-doped $Bi_2Sr_2Ca_2Cu_3O_x$ (Bi-2223) systems.

We have reported previous oxygen partial pressure measurements on the Y-123 and Nd-123 systems [1,2]. In these studies the oxygen content was varied in well-defined small increments by means of a coulometric titration technique, and the equilibrium partial pressure (fugacity) above the sample was established from EMF measurements [3]. This method is sensitive to detecting phase transformations, oxygen nonstoichiometry, and thermodynamic properties of Y-123 and RE-123 systems where the single phase homogeneity regions have a wide range of oxygen content in the condensed phase. It should be noted that the coulometric technique has been utilized in promising bismuth-cuprate perovskite systems where the single-phase homogeneity regions have a very narrow range of oxygen content [4,5,6].

The transition temperatures have been reported to be about 90 K for (Y-123), 92 K for Gd-123, and 96 K for $NdBa_2Cu_3O_x$ (Nd-123), where x is close to the value of 7.00, with an oxygen deficiency x =~ 6.8. Note that ionic radii of trivalent Y, Gd, and Nd are 0.99, 1.02, and 1.10 Å, respectively [7], and that the transition temperature increases with increase of ionic radius. Between x = 6.5 and 7.0, the results of Veal et al. [8] for Y-123 showed two plateaus at 60 K and 90 K. It was postulated that the 60 K plateau (x =~ 6.63-6.80) characterizes the ortho-II structure and the 90 K plateau (x =~ 6.80-7.0) characterizes the ortho-I structure. The lower plateau was nearly absent for the case of Nd-123 [8,9].

It should be emphasized that unlike the Y-123 system, solubility of Nd in Ba and Gd in Ba has been observed for the Nd-123 and Gd-123 systems. According to Wu et al. [10], Gd-123 (solid solution) has a solubility limit of x = 0.2 in air, and the solubility limit can be reduced in low oxygen partial pressures resulting in precipitation of $GdBa_2CuO_5$ and CuO as second phases. It is thought that these dispersed phases can enhance the Jc of Re-123 type superconductors. However, compositional modulation between Nd and Ba sites in Nd-123 is thought to

improve flux pinning for large Jc instead of the presence of Nd-422 dispersed in the melt-processed Nd-123 matrix [11].

2. RESULTS AND DISCUSSION

Extensive EMF measurements were initially made at 600°C in order to establish whether the measurements were reversible with varying oxygen content. The results are shown in Fig. 1. As in the case of the Y-123 and Nd-123 systems previously reported [1,2], the EMF (and therefore the calculated oxygen partial pressure) showed reversible behavior for oxygen absorption and desorbtion over the composition range investigated. Temperature dependency measurements of oxygen partial pressure for selected compositions obtained from the coulometric titrations at 600°C were also carried out. The results are included in Fig. 1 (isotherms 400, 450 and 500°C). Typical examples of the reversible behavior of the
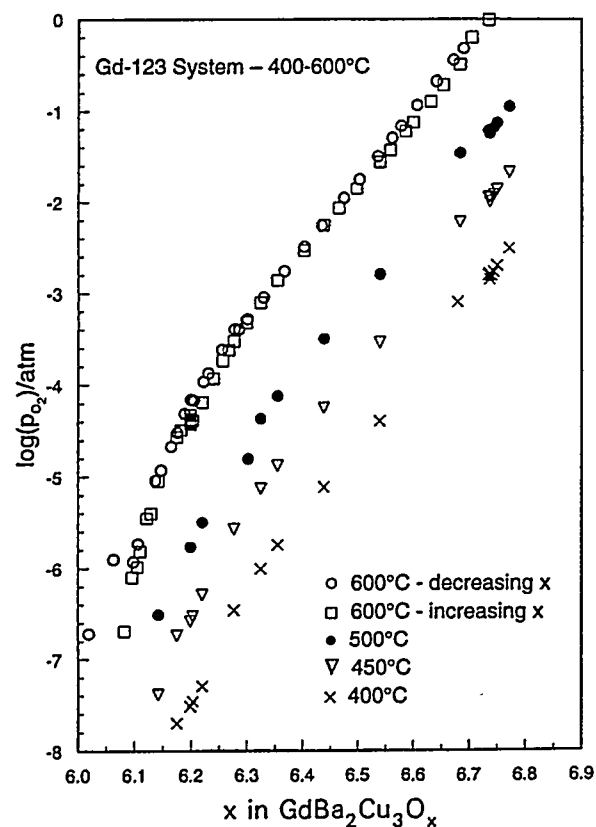
temperature dependency of oxygen partial pressure for a given oxygen content are shown in Figs. 2 and 3 for x = 6.18 and 6.33. Figure 4 shows an overview plot of the temperature dependencies of oxygen partial pressures for various oxygen coefficient values in the condensed phase of Gd-123 derived from our EMF measurements. It is readily seen that cooling these compositions at a fixed oxygen partial pressure increases the oxygen content of the condensed phase. Note that the absence of breaks in the temperature dependency plots indicates that Gd-123 is stable below the CuO/Cu_2O diphasic equilibrium line based on our measurements in the temperature range investigated. Oxygen partial pressures above coexisting pure CuO-Cu_2O phases [12] are included in the figures as broken lines. The EMF measurements of Bormann and Nolting [13] show that lead-free Bi-2212 and Y-Ba-Cu-O generally decompose very close to the CuO/Cu_2O boundary. It should be noted, however, that the TGA measurements of Feenstra et al. [14] on Y-123 thin

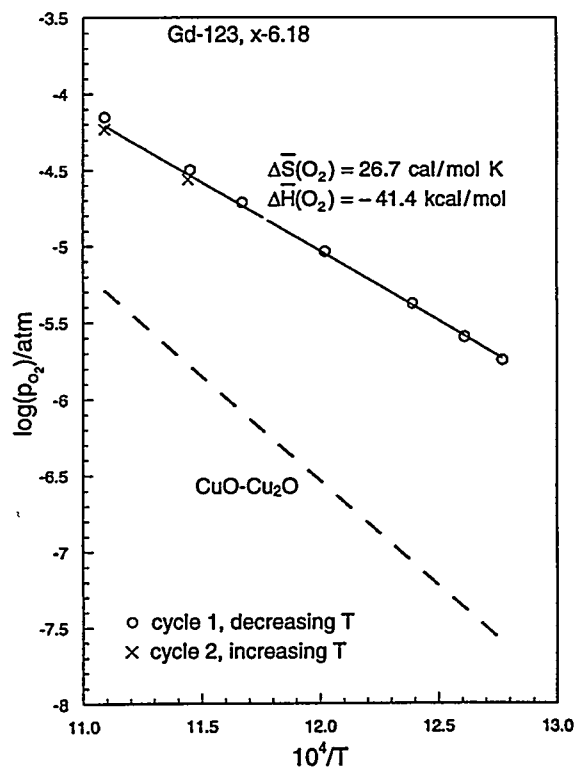Fig. 1. Variation of oxygen partial pressure with oxygen content and temperature.

Fig. 2. Temperature dependence of partial pressure of oxygen (x = 6.18).

films indicate that the material is stable to at least one order of magnitude lower pressure than the diphasic CuO/Cu_2O system.

Based on a least-square linear fit, and standard thermodynamic relationships, the slope of the temperature dependence of oxygen partial pressure for a given composition yields the partial molar enthalpy of solution of oxygen, $\Delta\overline{H}(O_2)$, and the intercept (at $1/T = 0$) determines the partial molar entropy of solution, $\Delta\overline{S}(O_2)$, in the Gd-123 compositions. The values are shown in Figs. 2 and 3. Because of space limitations, an assessment of the variation of these partial molar quantities with oxygen stoichiometry will be given in a later paper.
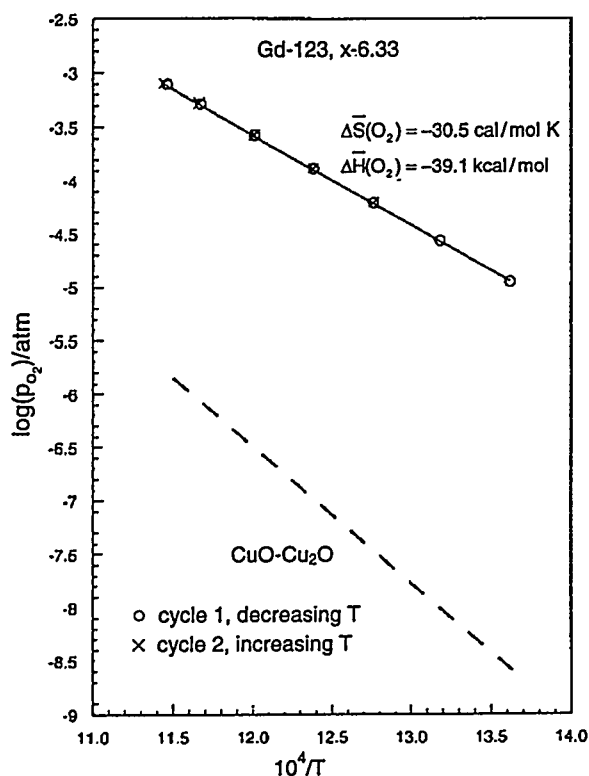

Fig. 3. Temperature dependence of partial pressure of oxygen (x = 6.33).

Equations for the variation of oxygen partial pressure with composition and temperature are given in Table 1 for selected compositions. These equations can serve as a basis for the optimized preparation and subsequent behavior of Gd-123 materials when exposed to various oxygen partial pressures and tem-

peratures. It should be recognized that control of oxygen content can be an important factor for achieving pinning properties that can result in increased Jc values.

Fig. 5 shows a comparison of oxygen partial pressure values as a function of oxygen stoichiometry for Y-123, Gd-123, and Nd-123 cuprate systems at 400°C. For a given oxygen stoichiometry, oxygen partial pressures above Gd-123 and Nd-123 are higher (above x = 6.5) than those for the Y-123 system, and appear to reflect the effect of the solubility of the rare earth atoms, Nd and Gd in Ba. According to Shaked et al. [15], the repulsion energy of oxygen atoms in O1 and O5 lattice sites in Nd-123 (and therefore also in the Gd-123 O1 and O5 lattice sites) is smaller than in Y-123. This lower repulsion energy apparently stabilizes the orthorhombic structure at higher values of x in Nd-123 and Gd-123 compositions compared to Y-123 as indicated in Fig. 5.
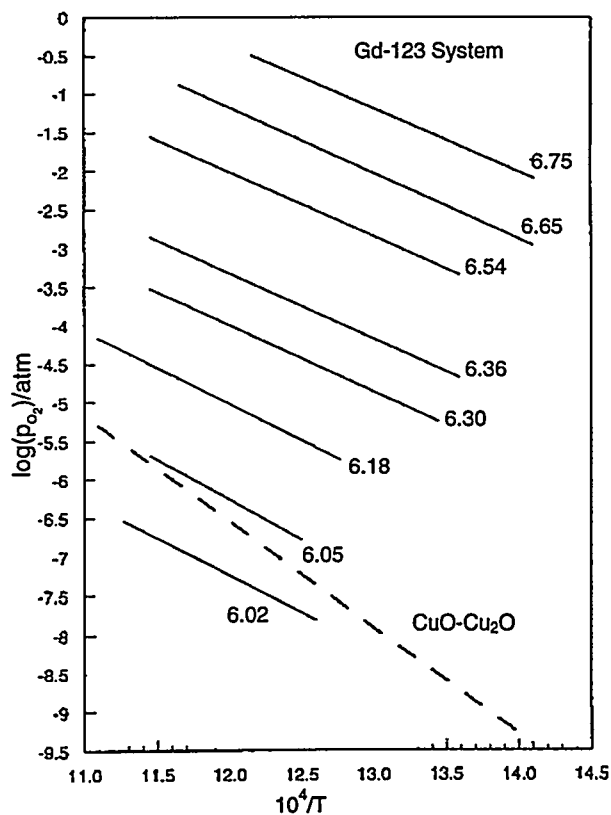

Fig. 4. Temperature dependence of partial pressure of oxygen (overview plot).

Table 1.

Equations for oxygen partial pressure above
$GdBa_2Cu_3O_x$ (400-600°C)
$\log p(O_2)/atm = A/T(K) + B$

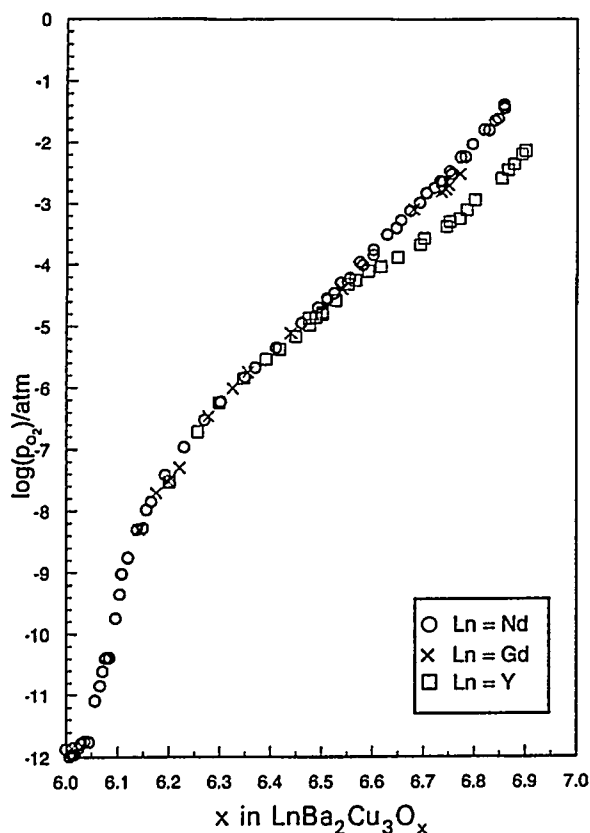| O_x	A	B
6.02	-9609	4.29
6.10	-112230	6.96
6.18	-94390	6.30
6.30	-8625	6.36
6.36	-8480	6.85
6.54	-8335	7.99
6.65	-8520	9.05
6.75	-8175	9.44

Fig. 5. Partial pressure of oxygen as a function of oxygen stoichiometry above Gd-123, Nd-123, and Y-123 systems at 400°C

SUMMARY

This paper presents thermodynamic properties that can be used to estimate the conditions of stability of the Gd-123 system as a function of temperature, oxygen partial pressure, and oxygen stoichiometry of the condensed phases. Equations for the variation of oxygen partial pressure derived from our EMF measurements can serve as a basis for the optimized preparation and subsequent behavior of Gd-123 compositions. Key findings of our measurements on the Gd-123 system are (1) Single phase stability regions have a wide range of oxygen stoichiometry for isotherms in the temperature range 400-600°C similar to results obtained with Y-123 and Nd-123 systems. (2) For a given oxygen stoichiometry, oxygen partial pressures above Gd-123 and Nd-123 are higher (above x = 6.5) than that for the promising Y-123 system. (3) In contrast to the BiSrCaCuO system and in general accord with the Y-123 system, our measurements show that Gd-123 is stable below the CuO/Cu_2O diphasic equilibrium line at low oxygen partial pressures in the temperature range 400-600°C.

REFERENCES

1. M. Tetenbaum, B. Tani, B. Czech, and M. Blander, Physica C 158 (1989) 377.
2. M. Tetenbaum, P. Tumidajski, D. L. Brown, and M. Blander, Physica C 198 (1992) 109.
3. Tretyakov and R. A. Rapp, Trans. Met. Soc. of AIME 245 (1969) 1235.
4. M. Tetenbaum, M. Hash, B. S. Tani, J. S. Luo, and V. A. Maroni, Physica C 249 (1995) 396.
5. M. Tetenbaum and V. A. Maroni, Physica C 260 (1996) 71.
6. M. Tetenbaum, M. Hash, B. S. Tani, and V. A. Maroni, Physica C 270 (1996) 114.
7. R. D. Shannon, Acta Crystallogr. A32 (1976) 75.

8. B. W. Veal, A. P. Paulikas, J. W. Downey, H. Claus, K. Vandervoort, G. Tomlins, H. Shi, M. Jensen, and L. Morss, Physica C 162-164 (1989) 97.

9. R. Nagarajan, R. Vijayaraghavan, R. A. Mohan Ram, and C. N. R. Rao, Physica C 158 (1989) 453.

10. H. Wu, M. J. Kramer, K. W. Dennis, and R. W. McCallum, IEEE Transactions on Applied Superconductivity, 7 (1997) 1731.

11. S. I. Yoo, N. Sakai, H. Takaichi, T. Higuchi, and M. Murakami, Appl. Phys. Lett. 65 (1994) 635.

12. R. A. Rapp and D. A. Shores, in Solid Electrolyte Cells in Physicochemical Measurements in Metal Research, Vol. 4, Part 2, Ed., R. A. Rapp, Interscience Publishers, New York (1970) 159.

13. R. Bormann and J. Nolting, Physica C 162-164 (1989) 81.

14. R. Feenstra, T. B. Lindemer, J. D. Budai, and M. D. Galloway, J. Appl. Phys. 69 (1991) 6569.

15. H. Shaked, B. W. Veal, J. Faber Jr., R. L. Hitterman, U. Balachandran, G. Tomlins, H. Shi, L. Morss, and A. P. Paulikas, Phys. Rev. B 41 (1990) 4173.